A&A 625, C1 (2019)
https://doi.org/10.1051/0004-6361/201833399e

Astronomy & Astrophysics

Nowhere to Hide: Radio-faint AGN in GOODS-N field

I. Initial catalogue and radio properties
(Corrigendum)

J. F. Radcliffe[1,2,3], M. A. Garrett[2], T. W. B. Muxlow[2], R. J. Beswick[2], P. D. Barthel[1], A. T. Deller[4], A. Keimpema[5], R. M. Campbell[5], and N. Wrigley[2]

[1] Kapteyn Astronomical Institute, University of Groningen, 9747 AD Groningen, The Netherlands
e-mail: j.f.radcliffe@astro.rug.nl
[2] Jodrell Bank Centre for Astrophysics/e-MERLIN, The University of Manchester, M13 9PL, UK
[3] ASTRON, the Netherlands Institute for Radio Astronomy, Postbus 2, 7990 AA Dwingeloo, The Netherlands
[4] Centre for Astrophysics and Supercomputing, Swinburne University of Technology, PO Box 218, Hawthorn, VIC 3122, Australia
[5] Joint Institute for VLBI ERIC, Postbus 2, 7990 AA Dwingeloo, The Netherlands

A&A, 619, A48 (2018), https://doi.org/10.1051/0004-6361/201833399

Key words. catalogs – radio continuum: galaxies – galaxies: active – galaxies: nuclei – techniques: high angular resolution – errata, addenda

We discovered an error in the coding for the expression calculating the radio power, $L_{1.5\,\mathrm{GHz}}$. In the original manuscript, the radio power was calculated using the VLA radio peak brightnesses whereas it should be calculated using the integrated flux densities. Whilst this makes little difference to compact sources, extended objects (e.g. J123656+615659, J123644+621133 and J123726+621129) had radio powers underestimated by up to an order of magnitude. This error has no significant effect upon the conclusions of the original manuscript. We outline where this error affects the original manuscript in the following couple of paragraphs.

Figure 6 and Table 3 are affected in the original manuscript and are corrected in this erratum. The online table at CDS has also been corrected.

On page 11, last sentence of the first paragraph should be: "As Fig. 6 shows, we sample a large range of radio powers from $\sim 10^{22}$–10^{26} W Hz^{-1} which have a median luminosity of 3.5×10^{24} W Hz^{-1}".

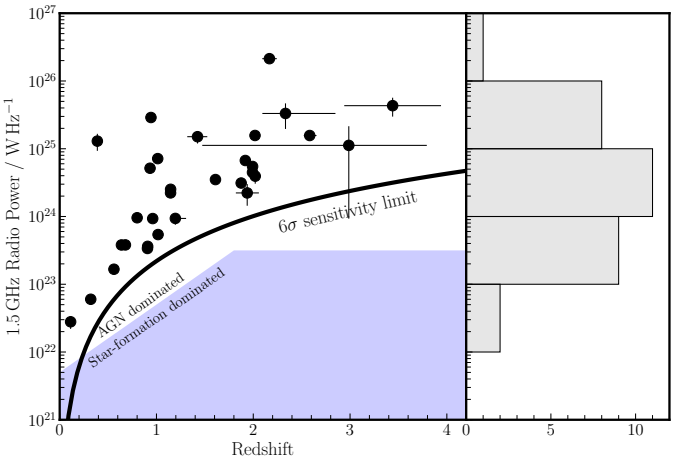

Fig. 6. Radio power vs. redshift for our VLBI sources. 1σ uncertainties on radio power and redshifts are plotted. The bold black curve represents the theoretical radio power that these VLBI observations are sensitive to (assuming all the VLA flux is contained in a milliarcsecond core) corresponding to $54\,\mu$Jy beam^{-1} or $6\times$ VLBI central rms The region above the blue shaded area represents the AGN dominated regime defined using the selection criteria of Magliocchetti et al. (2018). The histogram shows the distribution of the radio powers of which peak between 10^{24} and 10^{25} W Hz^{-1}.

Table 3. Derived VLA and VLBI radio properties of the 31 GOODS-N AGN.

Source ID	α	$L_{1.5\,\mathrm{Hz}}$ (W Hz^{-1})	T_b (K)	Angular sizes (mas)	Linear sizes (parsec)
(1)	(21)	(22,23)	(24–26)	(27–30)	(31–34)
J123555+620902	–	$(3.1 \pm 0.3) \times 10^{24}$	–	–	–
J123607+620951	−1.02	$(3.8 \pm 0.3) \times 10^{23}$	–	–	–
J123608+621036	−0.46	$(3.8 \pm 0.4) \times 10^{23}$	*1 × 10^6*	11.1 × 6.3	80.8 × 45.8
J123618+621541	−0.62	$(5.5 \pm 0.5) \times 10^{24}$	$>3 \times 10^7$	3.7 × <2.8	31.5 × <23.8
J123620+620844	−0.28	$(5.4 \pm 0.7) \times 10^{23}$	$>2 \times 10^7$	<3.2 × <2.8	<26.3 × <22.9
J123621+621708	−0.78	$(4.5 \pm 0.4) \times 10^{24}$	–	–	–
J123623+620654	0.06	$(2.2 \pm 0.8) \times 10^{24}$	–	–	–
J123624+621643	−0.52	$(6.7 \pm 0.7) \times 10^{24}$	2×10^7	5.9 × 4.0	50.9 × 34.1
J123641+621833	−0.94	$(2.2 \pm 0.2) \times 10^{24}$	*3 × 10^6*	12.3 × 5.0	104.4 × 42.6
J123642+621331	−1.05	$(1.6 \pm 0.1) \times 10^{25}$	*3 × 10^6*	12.1 × 8.5	103.4 × 73.2
J123644+621133	−0.56	$(7.1 \pm 0.7) \times 10^{24}$	$>1 \times 10^8$	2.1 × <1.7	17.6 × <13.9
J123646+621405	−0.40	$(9.3 \pm 1.1) \times 10^{23}$	$>2 \times 10^7$	<2.9 × <2.5	<23.9 × <20.1
J123650+620738	−0.56	$(3.5 \pm 0.4) \times 10^{24}$	–	–	–
J123653+621444	−0.11	$(6.0 \pm 0.8) \times 10^{22}$	*2 × 10^6*	9.2 × 4.8	44.1 × 23.0
J123659+621833	−1.19	$(2.1 \pm 0.1) \times 10^{26}$	$>1 \times 10^9$	6.2× < 0.9	52.3 × <7.7
J123700+620910	−0.89	$(1.6 \pm 0.1) \times 10^{25}$	*5 × 10^6*	9.5 × 7.2	78.3×59.1
J123709+620838	0.15	$(3.4 \pm 0.6) \times 10^{23}$	*2 × 10^6*	7.8 × 6.1	63.0 × 49.1
J123714+621826	−0.66	$(4.3 \pm 1.3) \times 10^{25}$	$>2 \times 10^8$	3.8×<1.7	28.5 × <12.9
J123715+620823	−0.04	$(5.2 \pm 0.8) \times 10^{24}$	$>3 \times 10^9$	<1.0 × <0.8	<7.9 × <6.9
J123716+621512	−0.19	$(1.7 \pm 0.2) \times 10^{23}$	*2 × 10^6*	10.4 × 6.5	69.1 × 43.4
J123717+621733	−0.89	$(2.5 \pm 0.2) \times 10^{24}$	*7 × 10^6*	6.8 × 5.1	57.6 × 43.2
J123720+620741	−0.28	$(3.6 \pm 0.6) \times 10^{23}$	–	–	–
J123721+621130	0.01	$(3.9 \pm 0.9) \times 10^{24}$	$>9 \times 10^7$	2.8 × <1.9	24.0 × <16.5
J123726+621129	−1.23	$(2.9 \pm 0.2) \times 10^{25}$	*2 × 10^6*	8.7 × 6.9	71.0 × 56.1
J123649+620439	–	$(2.8 \pm 0.6) \times 10^{22}$	–	8.4 × 6.0	17.7 × 12.7
J123701+622109	–	$(9.6 \pm 1.0) \times 10^{23}$	–	9.4 × 7.3	72.9 × 56.7
J123739+620505	–	$(1.1 \pm 1.0) \times 10^{25}$	–	8.6 × 7.2	68.0 × 56.6
J123751+621919	–	$(9.4 \pm 1.8) \times 10^{23}$	–	–	–
J123523+622248	–	$(1.5 \pm 0.3) \times 10^{25}$	–	–	–
J123510+622202	–	$(3.3 \pm 1.4) \times 10^{25}$	–	–	–
J123656+615659	–	$(1.3 \pm 0.4) \times 10^{25}$	–	7.3 × <2.4	39.6 × <13.2

Notes. α: 1.5 GHz–5.5 GHz spectral index, $L_{1.5\,\mathrm{GHz}}$: monochromatic 1.5 GHz radio luminosity, T_b: brightness temperature (italicised indicates that natural weighting was used to derive T_b), Angular size: projected angular size using elliptical Gaussian fitting, Linear size: projected linear size in parsecs. Italiscised source IDs correspond to sources with no-primary beam correction applied. Row of numbers below the column titles correspond to the columns in the machine-readable table that accompanies this paper.

References

Magliocchetti, M., Popesso, P., Brusa, M., & Salvato, M. 2018, MNRAS, 473, 2493